# LONG-TERM DYNAMICAL EVOLUTION OF HIGH AREA-TO-MASS RATIO DEBRIS RELEASED INTO HIGH EARTH ORBITS

Luciano Anselmo and Carmen Pardini – Space Flight Dynamics Laboratory, ISTI/CNR, Pisa, Italy


## ABSTRACT

The long-term dynamical evolution of objects with extremely high area-to-mass ratios released in synchronous and semi-synchronous orbits was simulated with a numerical propagator including all the relevant perturbations. In fact, as suggested by optical observations in the geosynchronous regime and orbital analysis of breakup fragments in low Earth orbit, artificial debris characterized by area-to-mass ratios hundreds or thousands of times greater than those of intact satellites or rocket bodies might be produced much more frequently than previously supposed. The results obtained show that even objects with area-to-mass ratios of tens of $m^2/kg$ may remain in space for several decades, or more, with very wide eccentricity excursions and orbit pole precessions, but maintaining a mean motion close to the original one, either synchronous or semi-synchronous.


## INTRODUCTION

Optical observations have led to the discovery of a population of faint uncataloged objects, with mean motions of about 1 revolution per day and orbital eccentricities as high as 0.8 [1] [2] [3]. The discovery of such objects was initially quite surprising, but an obvious explanation for their origin was immediately proposed. In fact, direct solar radiation pressure may significantly affect the eccentricity with small effects on the total energy of the orbit and, therefore, on the semi-major axis or mean motion. However, this perturbation would be adequately effective only on objects with sufficiently high area-to-mass ratios (A/M).

The existence of a substantial amount of orbital debris larger than 10 cm with A/M $\geq$ 1 $m^2/kg$, resulting from breakups or surface degradation, had not been previously anticipated, but a statistical analysis of the A/M distribution for the debris of the Fengyun-1C breakup has shown that about 5% of the cataloged fragments had A/M $\geq$ 1 $m^2/kg$ and slightly more than 1% had A/M $\geq$ 10 $m^2/kg$ (up to 90 $m^2/kg$) [4]. Therefore, the generation of orbital debris larger than 10 cm and with A/M hundreds or thousands of times greater than those of intact satellites might be more common than previously supposed, being one of the standard consequences of fragmentation events, both at high and low energy, involving spacecraft and rocket bodies with multi-layered insulation (MLI) blankets [5].

In low Earth orbit, below 1000 km, the orbital lifetime of such high A/M fragments would be relatively short compared to that of typical cataloged debris, due to the action of atmospheric drag. Even at higher altitudes the lifetime of high A/M objects would generally be shorter than the average, but in this case the driving perturbations would be direct solar radiation pressure and luni-solar third body attraction. However, depending on the initial conditions, quite long lifetimes become possible in high Earth orbits also for very high A/M objects, affecting the orbital debris environment for several decades or even more.

In order to grasp the long-term dynamical behavior in some high Earth orbits of interest and trace the possible origins of this unexpected (and still not fully uncovered) class of high A/M objects, a special perturbations propagator, using a high accuracy numerical integrator, was used to perform realistic simulations with a force model including the zonal and tesseral harmonics of the Earth's gravity potential, the luni-solar third body perturbation, the direct solar radiation pressure, with the Earth's shadow, and the thermospheric density for air drag computations, when appropriate. The results obtained for the synchronous and semi-synchronous orbital regimes are detailed in the following sections.

THE GEOSYNCHRONOUS ORBITAL REGIME

The computations were carried out by simulating the release in geostationary orbit, with a negligible relative velocity, of test objects with $C_R$ x A/M up to 60 $m^2/kg$ (were $C_R$ is a dimensionless radiation pressure coefficient, which typically assumes values between 1 and 2) [6] [7]. Eight release longitudes were chosen, four corresponding to the geopotential equilibrium points (two stable and two unstable) and the other four between them. The test objects were propagated for 54 years, a time span approximating the well-known precession period of the orbital plane of an abandoned geostationary spacecraft, with the force model described in the previous section. Concerning the Earth's gravity potential, the harmonics up to the eight degree and order were retained, while in case of induced high eccentricity orbits, with perigee altitude below 1000 km, the perturbing effects of air drag were considered as well, using the 1976 United States Standard Atmosphere [6] [7].

All objects with $C_R$ x A/M $<$ 45 $m^2/kg$ exhibited an orbital lifetime $>$ 54 years (the upper limit of the simulations), with a semi-major axis, and consequently a mean motion, close to the geosynchronous one. For $C_R$ x A/M $>$ 54 $m^2/kg$, the lifetimes resulted to be always $<$ 5 months, due to the rapid increase of the eccentricity and the ensuing Earth intercept [7]. In the transition region between 45 and 54 $m^2/kg$, a larger $C_R$ x A/M typically translated into a shorter lifetime, although the details of the evolution depended on the initial conditions. However, being the orbital decay usually induced by an eccentricity growth and a sudden decrease of the perigee height, the semi-major axis and the orbital period generally remained close to the geosynchronous ones until the actual Earth intercept [6] [7].

In order to give an idea of the main characteristics of the motion, the dynamical evolution over one century of an object with $C_R$ x A/M $\approx$ 20 $m^2/kg$, like some of those discovered in nearly geosynchronous orbit by optical observations [2], is presented in the following in terms of mean Keplerian elements [8]. The initial conditions are provided in Table 1.

Table 1: Release initial conditions in geosynchronous orbit of test object with $C_R$ x A/M = 20.4 $m^2/kg$

| | |
|---|---|
| Epoch | 2005.12.22 00:00 UTC |
| Orbital Elements | Mean Keplerian |
| Earth Centered Reference Frame | True of Date |
| Semi-major Axis | 42164.465 km |
| Eccentricity | 0.0001 |
| Inclination | 0.097° |
| Right Ascension of Ascending Node | 50.00° |
| Argument of Perigee | 220.00° |
| Mean Anomaly | 301.22° |

The evolution of the semi-major axis was mainly affected by the $J_{22}$ tesseral term of the geopotential and the combined action of direct solar radiation pressure and Earth's shadow, the latter two inducing a yearly oscillation [8]. However, during the time span of the simulation (100 years), the semi-major axis did not ever change by more than 0.8% with respect to the synchronous one [8].

Concerning the eccentricity, the geopotential harmonics alone induced very small short and long-term oscillations, mainly due to $J_2$, with amplitudes of about $6 \times 10^{-6}$ [8]. The addition of luni-solar third body attraction caused a long-term oscillation with an average period of 10.4 years and amplitude of about $6 \times 10^{-4}$ [8]. The inclusion of solar radiation pressure, on the other hand, induced a yearly oscillation with amplitude of about 0.4 and long period modulations of $\sim$ 0.05 (Figure 1) [8]. The evolution of the eccentricity vector was

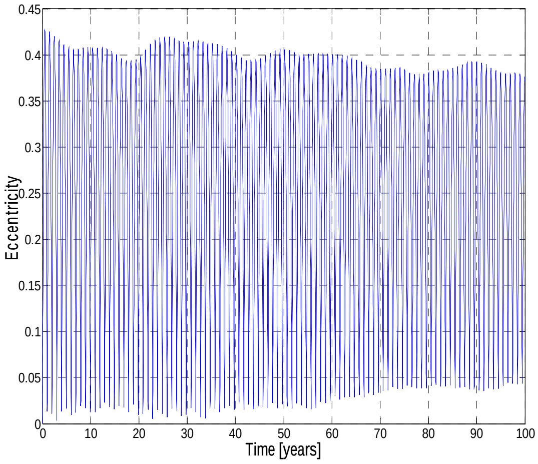


Figure 1: Eccentricity long-term evolution of test object released in geosynchronous orbit with $C_R$ x A/M = 20.4 $m^2$/kg.

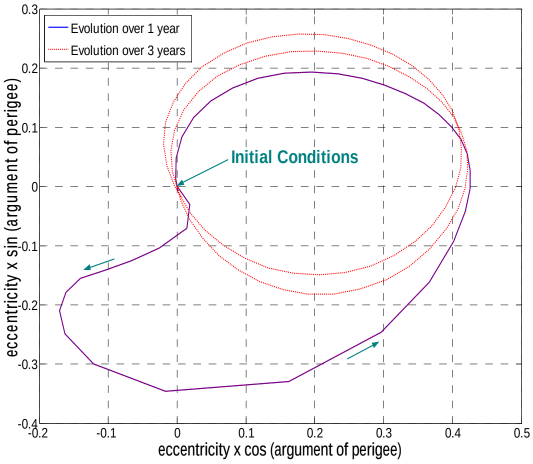


Figure 2: Eccentricity vector evolution over 3 yrs of test object released in geosynchronous orbit with $C_R$ x A/M = 20.4 $m^2$/kg.

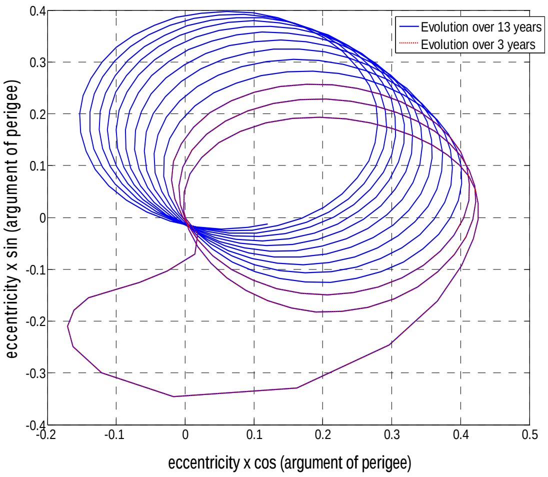


Figure 3: Eccentricity vector evolution over 13 yrs of test object released in geosynchronous orbit with $C_R$ x A/M = 20.4 $m^2$/kg.

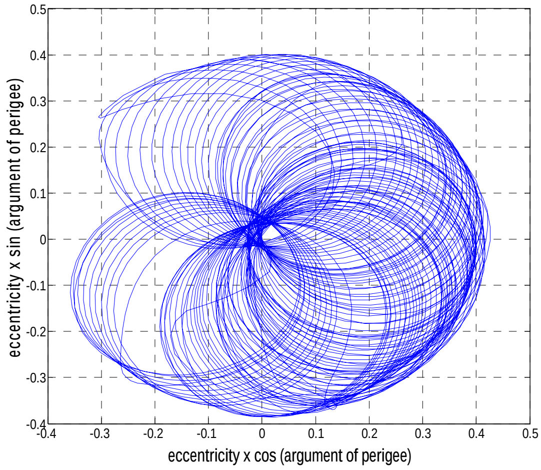


Figure 4: Eccentricity vector evolution over 100 yrs of test object released in geosynchronous orbit with $C_R$ x A/M = 20.4 $m^2$/kg.

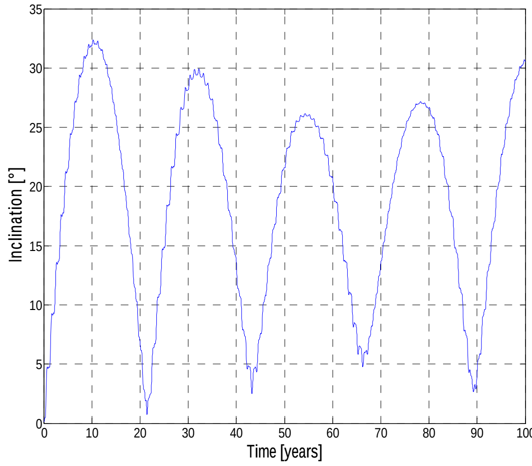


Figure 5: Inclination long-term evolution of test object released in geosynchronous orbit with $C_R$ x A/M = 20.4 $m^2$/kg.

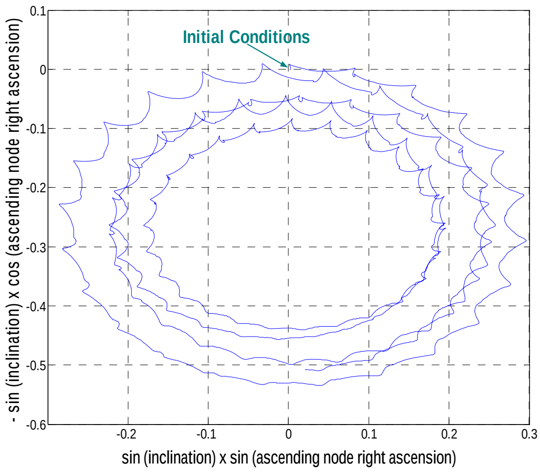


Figure 6: Inclination vector evolution over 100 yrs of test object released in geosynchronous orbit with $C_R$ x A/M = 20.4 $m^2$/kg.

basically characterized by the superimposition of two anti-clockwise precession motions, both with a radius of about 0.2 (Figures 2, 3 and 4). One precession cycle was completed in 1 year, while the other presented a significantly longer period and a more complex behavior [8].

Regarding the inclination evolution, the geopotential effects were negligible. Only the right ascension of the ascending node was subjected to a regression of –0.0134° per day, largely due to $J_2$. The addition of luni-solar perturbations, on the other hand, induced the well-known clockwise precession of the orbit angular momentum vector, with a period of 53.3 years and amplitude of about 15° (corresponding to the value of the maximum inclination). However, with a so high area-to-mass ratio ($C_R$ x A/M = 20.4 $m^2$/kg), the inclusion of direct solar radiation pressure resulted into a quite complex evolution [8]. The inclination presented oscillations of varying amplitude, reaching a maximum value of 32.4° (Figure 5). The average period of these oscillations was about 22.4 years. The evolution of the orbit pole consisted of a clockwise precession motion, characterized by the same varying amplitude and duration of the dominant inclination oscillation (Figure 6). A smaller wobbling motion, with amplitude of about 1° and period of approximately 1 year, was superimposed to the main long-term precession [8].

In general, it was found that the eccentricity evolution was dominated by yearly oscillations with much smaller long period modulations. Increasing $C_R$ x A/M from 1 to 48 $m^2$/kg, the amplitude of the yearly eccentricity oscillation grew from 0.02 to 0.8, while the long period modulation grew from $\sim$ 0.002 to $\sim$ 0.05 [7].

Concerning the orbit plane evolution, objects with $C_R$ x A/M up to 1 $m^2$/kg presented the classical behavior of typical abandoned geostationary spacecraft, with a maximum inclination of nearly 15° and an orbit pole precession period of about 53 years. An increase in the area-to-mass ratio resulted into a faster and wider orbit pole clockwise precession. For objects with $C_R$ x A/M = 48 $m^2$/kg, one orbit pole precession cycle was completed in about 5.4 years, with a maximum inclination of approximately 48° [7].

## THE GPS ORBITAL REGIME

The computations were carried out by simulating the release, in each of the six orbital planes used by the Block II satellites of the Global Positioning System (GPS), of test objects with $C_R$ x A/M up to 120 $m^2$/kg [9]. The orbital state vectors of six operational satellites, one for each plane, were chosen as initial conditions, assuming a negligible release velocity. The test objects were propagated for 100 years, taking into account the geopotential harmonics up to the 16$^{th}$ degree and order, luni-solar attraction and direct solar radiation pressure with eclipses. In case of induced high eccentricity orbits with perigee altitude below 1000 km, the perturbing effects of air drag were considered as well, using the 1976 United States Standard Atmosphere [9].

Disregarding the effects of solar radiation pressure, a detailed description of the basic properties of the GPS Block II orbits can be found elsewhere [9] [10] [11] [12]. Here is important to recall that these nearly circular orbits, with period equal to 1/2 of a sidereal day ($\approx$ 718 minutes), semi-major axis close to 26,560 km and inclination of about 55°, are in deep 2:1 resonance with the Earth's rotation. The ascending nodes of the six planes are separated by 60° in right ascension and each plane is identified by a capital letter, from A to F, while the satellites in each plane are identified by a number. Due to the ground track geometry and repeat frequency, the most important geopotential resonant term affecting the semi-major axis is $J_{32}$, leading to the existence of stable (28°E, 208°E) and unstable (118°E, 298°E) longitudes of the ascending node [10]. This results in a nearly harmonic motion around the stable points, in the phase plane defined by the longitude of the ascending node and the semi-major axis [10] [13]. The period of small amplitude motion is about 8.4 years, increasing to about 14 years far away from the stable equilibrium points [9].

Concerning the orbital lifetime of high area-to-mass ratio objects, all those analyzed with $C_R$ x A/M up to 54 $m^2$/kg exhibited a lifetime greater than 35 years (very often greater than 100 years), with semi-major axis and orbital period remaining close to the semi-synchronous values [9]. For 54 $m^2$/kg $<$ $C_R$ x A/M $<$ 96 $m^2$/kg, the exact value depending on the initial conditions, the eccentricity became so large, and the perigee altitude so

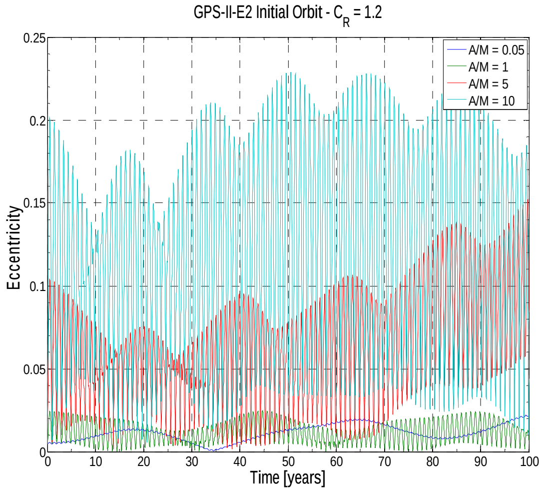


Figure 7: Eccentricity long-term evolution as a function of A/M (in m²/kg) assuming the E2 initial conditions.

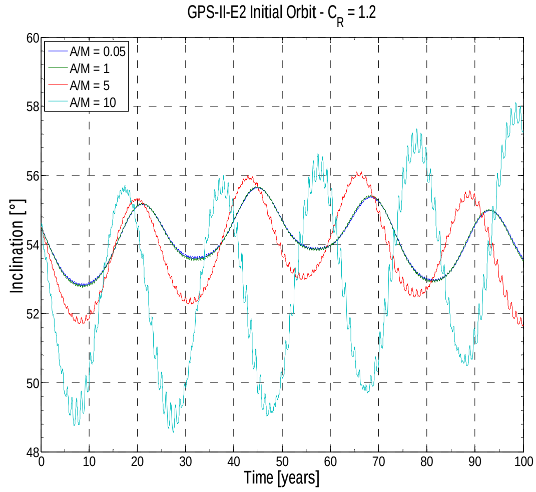


Figure 10: Inclination long-term evolution as a function of A/M (in m²/kg) assuming the E2 initial conditions.

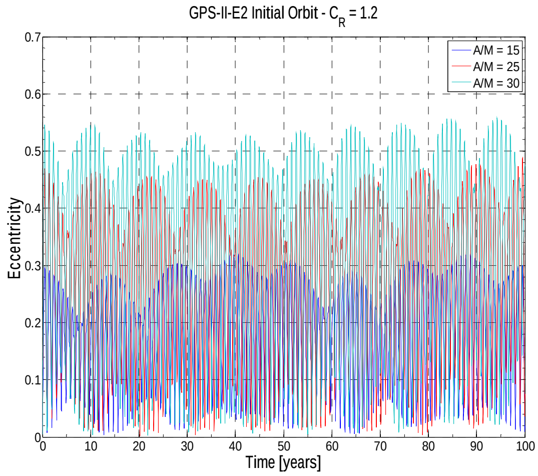


Figure 8: Eccentricity long-term evolution as a function of A/M (in m²/kg) assuming the E2 initial conditions.

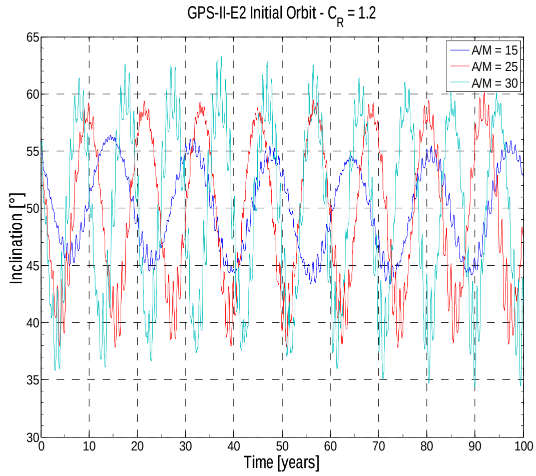


Figure 11: Inclination long-term evolution as a function of A/M (in m²/kg) assuming the E2 initial conditions.

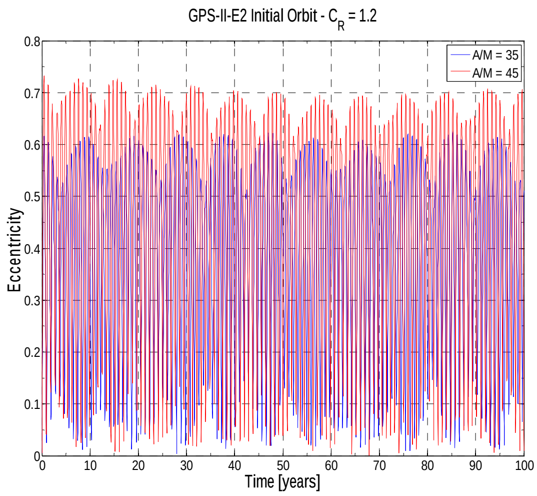


Figure 9: Eccentricity long-term evolution as a function of A/M (in m²/kg) assuming the E2 initial conditions.

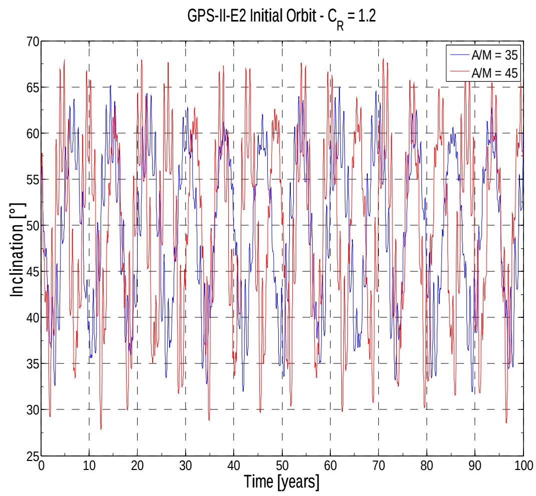


Figure 12: Inclination long-term evolution as a function of A/M (in m²/kg) assuming the E2 initial conditions.

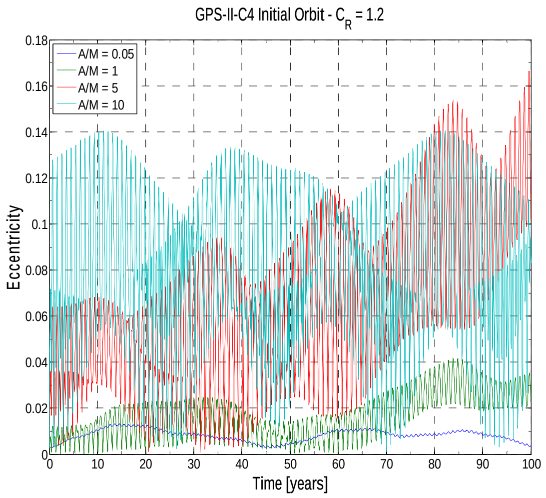


Figure 13: Eccentricity long-term evolution as a function of A/M (in m²/kg) assuming the C4 initial conditions.

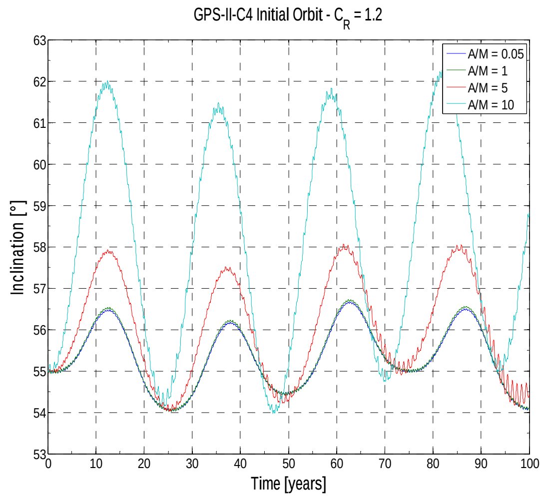


Figure 16: Inclination long-term evolution as a function of A/M (in m²/kg) assuming the C4 initial conditions.

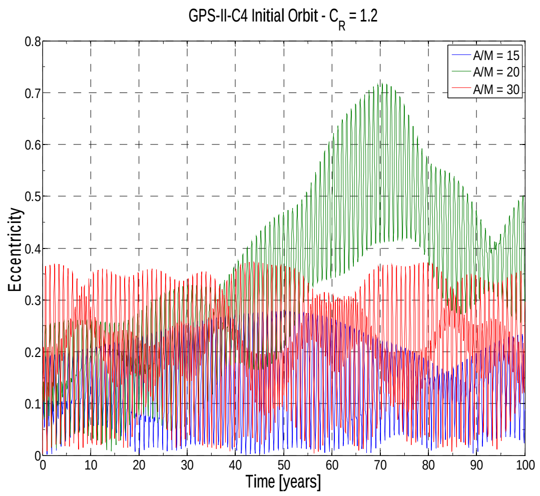


Figure 14: Eccentricity long-term evolution as a function of A/M (in m²/kg) assuming the C4 initial conditions.

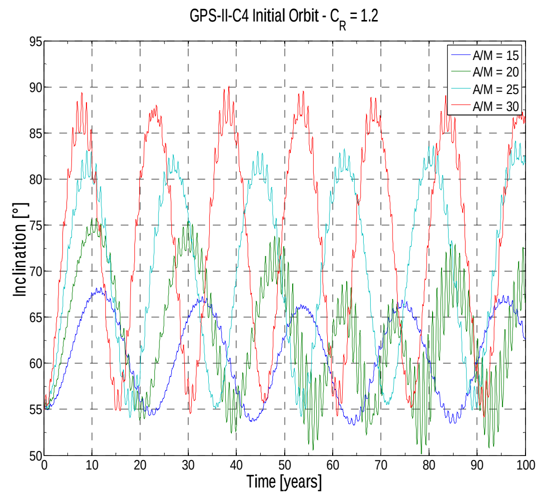


Figure 17: Inclination long-term evolution as a function of A/M (in m²/kg) assuming the C4 initial conditions.

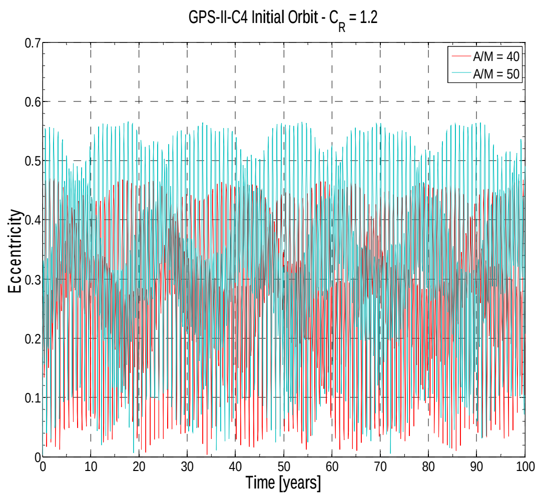


Figure 15: Eccentricity long-term evolution as a function of A/M (in m²/kg) assuming the C4 initial conditions.

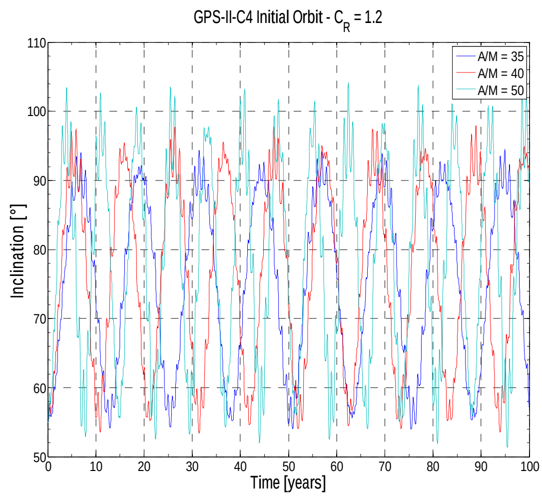


Figure 18: Inclination long-term evolution as a function of A/M (in m²/kg) assuming the C4 initial conditions.

low, that an orbital decay occurred in a few months. But even in these cases, the semi-major axis and the orbital period remained close to the semi-synchronous values until Earth intercept [9].

Regarding the long-term evolution of mean eccentricity and inclination, the results obtained with the E2 and C4 initial conditions (Table 2) are presented as an example in Figures 7-18, for a subset of $C_R$ x A/M values spanning the investigated range. E2 was characterized by initial conditions close to the stable equilibrium points in the phase plane defined by the longitude of the ascending node and the semi-major axis, while C4 was in an intermediate position [9].

Table 2: Release initial conditions of E2 and C4 test objects in semi-synchronous GPS orbits

| GPS Constellation Orbit Slot | E2 | C4 |
|---|---|---|
| Epoch | 2007.04.16 17:29 UTC | 2007.04.16 07:29 UTC |
| Orbital Elements | Mean Keplerian | Mean Keplerian |
| Earth Centered Reference Frame | True of Date | True of Date |
| Semi-major Axis | 26560.432 km | 26559.616 km |
| Eccentricity | 0.0048672 | 0.0026456 |
| Inclination | 54.5093° | 54.9919° |
| Right Ascension of Ascending Node | 312.7360° | 190.2977° |
| Argument of Perigee | 265.1898° | 189.3242° |
| Mean Anomaly | 94.2809° | 170.6826° |

The common feature of the evolution, which was shared by the other cases analyzed but not shown here, was that the semi-major axis remained close to the semi-synchronous value, even when the orbital decay was imminent due to the growth in eccentricity. In general, higher values of $C_R$ x A/M resulted in larger amplitudes of the yearly eccentricity oscillation due to direct solar radiation pressure (Figures 7, 8 and 9 for E2; Figures 13, 14 and 15 for C4). In the E2 case, for example, the maximum eccentricity was ~ 0.2 for $C_R$ x A/M ~ 10 $m^2/kg$, ~ 0.5 for $C_R$ x A/M ~ 30 $m^2/kg$ and ~ 0.7 for $C_R$ x A/M ~ 50 $m^2/kg$. However, certain initial conditions, coupled with luni-solar resonances, may change this simple behavior, adding to the yearly oscillation a term with significantly longer period and wider amplitude. In the C4 case, this can easily be seen in Figure 14 for $C_R$ x A/M = 24 $m^2/kg$, when the eccentricity peaked above 0.7.

The long-term behavior of the mean inclination is shown in Figures 10, 11 and 12 for E2 and in Figures 16, 17 and 18 for C4. For $C_R$ x A/M $\leq$ 1 $m^2/kg$, the evolution of the orbit plane was still dominated by the interaction between $J_2$ and the third body attraction, with the typical GPS Block II nodal regression period of $\approx$ 26 years and inclination oscillation amplitude of ~ 2°, superimposed on a longer term trend driven by luni-solar perturbations. An increase in $C_R$ x A/M had, as a consequence, a faster nodal regression and wider amplitude of the inclination excursion, with numbers depending on the initial conditions. In the E2 case, for example, $C_R$ x A/M $\approx$ 12 $m^2/kg$ induced an inclination oscillation amplitude of $\approx$ 7° and a nodal precession period of $\approx$ 20.6 years, $C_R$ x A/M $\approx$ 30 $m^2/kg$ induced an inclination oscillation amplitude of $\approx$ 20° and a nodal precession period of $\approx$ 11.7 years, and $C_R$ x A/M $\approx$ 48 $m^2/kg$ induced an inclination oscillation amplitude of $\approx$ 30° and a nodal precession period of $\approx$ 6.6 years. For sufficiently high $C_R$ x A/M values and specific initial conditions, the orbit became periodically retrograde (i.e. with inclination > 90°) for some time. For instance, this situation occurred with $C_R$ x A/M larger than ~ 40 $m^2/kg$ in the C4 case.

In conclusion, also in this orbital regime, as already found for geosynchronous objects, very long orbital lifetimes are possible, even with extremely high area-to-mass ratios. Depending on the initial conditions, eccentricities as high as 0.7 could be attained with 25 $m^2/kg \leq C_R$ x A/M $\leq$ 90 $m^2/kg$, maintaining, however, a semi-major axis and mean motion close to the semi-synchronous values. The inclination would also experience a wider excursion, associated with a faster regression of the ascending node, with increasing values of the area-to-mass ratio.

## CONCLUSIONS

Recent optical observations in the geosynchronous regime and orbital analysis of breakup fragments in low Earth orbit have show that artificial debris characterized by extremely high area-to-mass ratios, hundreds or thousands of times greater than those of intact satellites or rocket bodies, might be much more common than previously supposed, being probably one of the standard consequences of fragmentation events, both at high (explosions or collisions) and low (surface ageing) energy.

The comprehensive set of simulations carried out in the synchronous and semi-synchronous orbital regimes indicate that objects with $C_R$ x A/M up to ~ 50 $m^2$/kg might explain the recently discovered debris population with mean motions of about one revolution per day and orbital eccentricities as high as 0.8. Significant orbital lifetimes (several decades) characterize the evolution of objects with $C_R$ x A/M $\leq$ 45 $m^2$/kg, while for $C_R$ x A/M $>$ 45-55 $m^2$/kg, the exact value depending on the initial conditions, the orbital lifetime is reduced to a few months, at the most. In general, a growth of $C_R$ x A/M would have, as a consequence, a larger amplitude of the yearly oscillations that dominate the eccentricity evolution, in addition to a faster and wider orbit pole clockwise precession.

Long lifetime orbits, with mean motions of about 2 revolutions per day, would also be possible for debris with extremely high area-to-mass ratios released at GPS altitudes. Often the lifetime would exceed one century for $C_R$ x A/M up to ~ 55 $m^2$/kg, decreasing rapidly to a few months above such a threshold. However, the details of the evolution, which are conditioned by the complex interplay of solar radiation pressure and geopotential plus luni-solar resonances, depend on the initial conditions. Different behaviors are thus possible, as a 35-year lifetime for $C_R$ x A/M $\approx$ 30 $m^2$/kg or a more than 100-year lifetime for $C_R$ x A/M $\approx$ 90 $m^2$/kg [9]. In any case, objects like those discovered in synchronous orbits could also survive in this orbital regime, with semi-major axes close to the semi-synchronous values, with maximum eccentricities up to 0.7, and with significant orbit pole precessions (faster and wider for increasing values of $C_R$ x A/M), leading to inclinations between 30° and more than 90°.

## ACKNOWLEDGEMENTS

The results described in this paper were obtained within the framework of the ASI Contracts No. I/023/06/0 and I/046/07/0.

## REFERENCES

[1] Schildknecht, T., Musci, R., Ploner, M., Beutler, G., Flury, W., Kuusela, J., de Leon Cruz, J., de Fatima Dominguez Palmero, L. Optical observations of space debris in GEO and in highly eccentric orbits, *Adv. Space Res.*, 34, 901-911, 2004.
[2] Schildknecht, T., Musci, R., Flohrer, T. Properties of the high area-to-mass ratio space debris population at high altitudes, *Adv. Space Res.*, 41, 1039-1045, 2008.
[3] Agapov, V., Biryukov, V., Kiladze, R., Molotov, I., Rumyantsev, V., Sochilina, A., Titenko, V. Faint GEO objects search and orbital analysis, in: Proceedings of the Fourth European Conference on Space Debris, ESA SP-587, ESA Publications Division, Noordwijk, The Netherlands, pp. 119-124, 2005.
[4] Pardini, C., Anselmo, L. Assessment of the consequences of the Fengyun-1C breakup in low earth orbit, *Adv. Space Res.*, doi: 10.1016/j.asr.2009.04.014, 2009.

[5] Liou, J.-C., Weaver, J. K. Orbital evolution of GEO debris with very high area-to-mass ratios, *The Orbital Debris Quarterly News*, 8, Issue 3, pp. 6-7, 2004.
[6] Anselmo, L., Pardini, C. Orbital evolution of geosynchronous objects with high area-to-mass ratios, in: Proceedings of the Fourth European Conference on Space Debris, ESA SP-587, ESA Publications Division, Noordwijk, The Netherlands, pp. 279-284, 2005.
[7] Pardini, C., Anselmo, L. Long-term evolution of geosynchronous orbital debris with high area-to-mass ratios, *Trans. Japan Soc. Aero. Space Sci.*, 51, 22-27, 2008.
[8] Anselmo, L., Pardini, C. Long-term evolution of high earth orbits: Effects of direct solar radiation pressure and comparison of trajectory propagators, Technical Report 2007-TR-008, ISTI/CNR, Pisa, Italy, 29 March 2007.
[9] Anselmo, L., Pardini, C. Dynamical evolution of high area-to-mass ratio debris released into GPS orbits, *Adv. Space Res.*, 43, 1491-1508, 2009.
[10] Hugentobler, U. Astrometry and satellite orbits: Theoretical considerations and typical applications, Geodätisch-geophysikalische Arbeiten in der Schweiz, Vol. 57, Schweizerische Geodätische Kommission, Zürich, Switzerland, 1998.
[11] Ineichen, D., Beutler, G., Hugentobler, U. Sensitivity of GPS and GLONASS orbits with respect to resonant geopotential parameters, *Journal of Geodesy*, 77, 478-486, 2003.
[12] Beutler, G. Methods of celestial mechanics, Volume II: Application to planetary system, geodynamics and satellite geodesy, Springer, Berlin, Germany, 2005.
[13] Ely, T.A. Impact of eccentricity on East-West stationkeeping for the GPS class of orbits, in: Astrodynamics 1999, *Advances in the Astronautical Sciences*, Vol. 103, Part II, Univelt Inc. Publishers, San Diego, California, USA, pp. 1391-1408, 2000.